

## Estimation of depth of maximum by relative muon content in air showers with energy greater than 5 EeV measured by the Yakutsk array

Stanislav Knurenko<sup>a</sup> and Igor Petrov<sup>a,\*</sup>

<sup>a</sup>*Yu. G. Shafer Institute of Cosmophysical Research and Aeronomy,  
Lenin avenue 31, Yakutsk, Russia*

*E-mail: [knurenko@ikfia.ysn.ru](mailto:knurenko@ikfia.ysn.ru), [igor.petrov@ikfia.ysn.ru](mailto:igor.petrov@ikfia.ysn.ru)*

Characteristics of muons with a threshold  $\varepsilon_{thr} \geq 1$  GeV based on the air showers data in Yakutsk array were analyzed. Quantitative estimation of muons at different distance from the shower axis and the ratio of muon and charged particles at a distance of 600 m are obtained. An empirical relationship between the fraction of muons and longitudinal development — the depth of maximum development  $X_{max}$  is found. Calculations of the muon fraction are performed using the QGSjetII-04 for different primary nuclei, and compared with experiment. Mass composition of primary particles induced air showers of highest energies is estimated from the muon component.

*37<sup>th</sup> International Cosmic Ray Conference (ICRC 2021)  
July 12th – 23rd, 2021  
Online – Berlin, Germany*

---

\*Presenter

## 1. Introduction

Despite the fact that cosmic rays (CR) have been measured up to energies of  $\sim 200$  EeV, their sources have not yet been established, and the mechanisms of generation and acceleration of primary particles and their mass composition (MC) have not been studied [1–5]. According to recent observations, possible CR sources in this energy range might be: cosmic bubble structures [6], supernova remnants, compact jets of active galactic nuclei [7], galaxy clusters [8], radio galaxies [9] and gamma-ray bursts [10]. In turn, CRs can be divided according to their energy into galactic  $E < 0.1$  EeV and extragalactic  $E \geq 0.1$  EeV. The characteristics of CRs in this energy range are not yet precisely known and, for this reason, are the subject of their study at small, medium, and large arrays of extensive air showers. The recently obtained irregularity in the CR spectrum at an energy of  $\sim 0.1$  EeV [11–13], associated with the rigidity of particles of galactic origin, is of even greater interest, since it opens up the possibility of determining the boundary of the transition from galactic to extragalactic CRs [14]. Knowledge of the MC of cosmic rays in the energy range 0.1-10 EeV is going to help to find the solution of this problem [15–17].

The CR composition has been directly measured only up to energies 100 TeV in experiments on satellites and balloons [18–25]. At higher energies, the MC is studied at air shower experiments by indirect methods, analyzing the longitudinal development of individual showers [26–29] and the integral characteristics of showers at sea level [30–33]. The results obtained indirectly largely depend on the experimental equipment, the atmospheric conditions under which the measurements are carried out, the methods for processing experimental data, the model of hadronic interactions, and other factors. Therefore, in order to verify the previously obtained results, it is important to obtain data on the MC using a different technique and another air shower component, for example, muons. It is known that the muon component is sensitive to the MC of the primary particles [34]. This is shown by calculations based on the QGSjetII-04 model [35] for a primary proton and an iron nucleus. Calculations have shown that a joint analysis of muons with the longitudinal development of air showers is capable of providing a reliable estimate of the MC of cosmic rays. And with reliable measurements, it is even possible to separate the primary particles that produces air shower according to their atomic weight [32, 33].

## 2. Experimental data on the air shower muon component. Comparison with calculations

The cascade process of muon production in the atmosphere depends on the point of the first interaction of the primary nucleus with air atoms and ionization losses per unit path of the particle. For a heavy nucleus, the point of the first interaction will be higher in the atmosphere than for a light nucleus. Because of this, the air shower will begin to develop earlier and the shower development maximum  $X_{\max}$  will be higher in the atmosphere. Due to the difference in the absorption paths of the muon and electron-photon components at sea level, the fraction of muons  $\rho_{\mu}(600)/\rho_{\mu+e}(600)$  will be larger for heavy nuclei and less for light nuclei. As shown in [36], showers from protons and iron nuclei are concentrated in different intervals in  $X_{\max}$ . Therefore, the most sensitive parameter to  $X_{\max}$ , and hence to MC, will be the fraction of muons  $\rho_{\mu}(600)/\rho_{\mu+e}(600)$ . It is the ratio of the

muon flux density  $\rho_\mu(600)$  to the charged particle flux density  $\rho_{\mu+e}(600)$ , which for this work was taken at a distance of 600 m from the air shower axis.

Over 20 years of continuous observations, 1995-2015, more than  $10^6$  EAS events with data on the muon component and energies above 50 PeV were recorded at the Yakutsk array. For the analysis, 802 showers with energies  $E_0 \geq 5$  EeV and zenith angles  $\theta \leq 60^\circ$  were selected. Air shower events with energies above 10 EeV accounted for 25 % of the total number of showers included in the sample. The sample of showers was formed according to the following criteria: showers' axes lie within a circle with a radius of 1000 m from the center of the array; there are measurements of muons in the range of distances of 300-800 m; The accuracy of determining the axis in showers was (10-20) m along the  $x_0$  axis, and (15-25) m along the  $y_0$  axis. The accuracy of determining the density of charged particles and muons at a distance of 600 m was  $\sim (10-15)\%$ . In this case, approximately the same conditions for the registration of showers and close in values of the measurement accuracy of the main characteristics of air shower were realized. By measuring the flux of charged particles and muons, the classification parameters  $\rho_{\mu+e}(600)$  and  $\rho_\mu(600)$  were determined.

The shower energy  $E_0$  was determined from the measured muon flux density  $\rho_\mu(600)$  by formula (1) [30].

$$\log_{10} E_0 = 18.33 + 1.12 \cdot \log_{10}(\rho_\mu(R = 600, \theta)) \quad (1)$$

## 2.1 Estimation of the Depth of the air shower Development Maximum from the Muon Component

In individual showers, where the EAS Cherenkov light, charged particles and muons were measured, the classification parameters  $\rho_\mu(600)$  and  $\rho_{\mu+e}(600)$  were found, and the depth of the maximum development  $X_{\max}$  was reconstructed from the lateral distribution of Cherenkov light [37–39]. Next, we compared parameter  $\rho_\mu(600)/\rho_{\mu+e}(600)$  with  $X_{\max}$  for three zenith angles (Fig. 1). Figure 1 shows averaged data and QGSjetII-04 calculations for zenith angles  $\langle\theta\rangle = 18^\circ$ ,  $\langle\theta\rangle = 38^\circ$  and  $\langle\theta\rangle = 58^\circ$ , dashed curves. Simulations are performed with CORSIKA [40] with thinning ( $10^{-5}$ ). The simulation took into account the response of a scintillation detector with a threshold of 10 MeV and its fluctuations [41]. As can be seen in the Fig. 2, there is a discrepancy between experiment and simulations for large and small values of  $X_{\max}$  for all zenith angles. It might be related to muon deficit in hadronic models [42]. Solid curves are approximations (2):

$$X_{\max} = A_1 \cdot \left( -\frac{\rho_\mu/\rho_{\mu+e}}{t_1} \right) + y_0 \quad (2)$$

The coefficients  $A_1$ ,  $t_1$ , and  $y_0$  were determined by the approximation of the experimental data by function (2).

As follows from the analysis, the coefficients in equation (2) depend only on the length of the muon track in the atmosphere. The generalized formula connecting  $X_{\max}$  with the ratio  $\rho_\mu(600)/\rho_{\mu+e}(600)$  is expressed as:

$$X_{\max} = (535 + 2887 \cdot (\sec \theta - 1)) \cdot \exp \left( -\frac{(\rho_\mu/\rho_{\mu+e})\theta}{0.521 + 3.980 \cdot (\sec \theta - 1)} \right) + (386 - 2524(\sec \theta - 1)) \quad (3)$$

Formula (3) was used to estimate  $X_{\max}$  in individual showers from the measured muon component of the air shower.

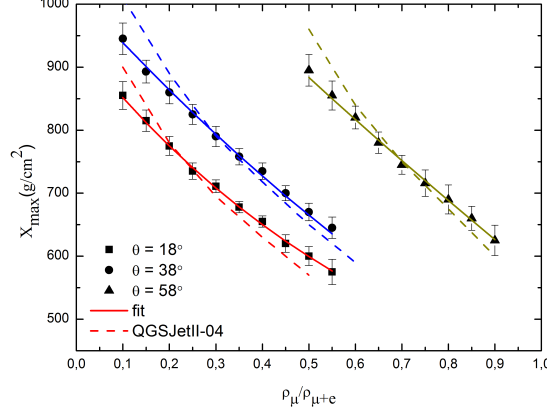


**Figure 1:** Relationship between the depth of the maximum of the electromagnetic cascade and the fraction of muons at a distance of 600 m from the shower axis. Solid curves — fit, dashed curves — calculation using the QGSjetII-04 hadron interaction model for zenith angles  $\langle\theta\rangle = 18^\circ$ ,  $\langle\theta\rangle = 38^\circ$  and  $\langle\theta\rangle = 58^\circ$ , respectively.

## 2.2 Dependence of $X_{\max}$ on $E_0$ in the region of highest energies

$X_{\max}$  was estimated by formula (3) in individual showers with energies greater than 5 EeV by fraction of muons at a distance of 600 m. The data was binned into several energy intervals and the  $\langle X_{\max} \rangle$  was determined for each interval. In these intervals, fluctuations were also estimated. To estimate the physical fluctuations in the development of air shower  $\sigma(X_{\max})$ , we used the fluctuations of measurements of  $\sigma(X_{\max})_{meas}$  and instrumental errors  $\sigma(X_{\max})_{app}$ , which were obtained in the course of simulating measurements of muons and charged particles at the Yakutsk [26]:

$$\sigma^2(X_{max}) = \sigma^2(X_{max})_{meas} - \sigma^2(X_{max})_{app} \quad (4)$$

The results are shown in Fig. 2, red triangles. Since only a part of the showers with muons was considered, the result obtained can be considered as preliminary. For comparison, Fig. 2a shows the data of the Yakutsk array for other components: the Cherenkov light [26], scintillation detectors, muon LDF component [43] and the radio emission [44, 45]. Also, the figure shows the data of the Auger [46, 47], Telescope array [48, 49], LOFAR [50] experiments and simulations: QGSJETII-04 [35], Sibyll 2.3c [51], EPOS-LHC [52]. The results of all settings within the measurement errors are in good agreement with each other and reflect the uneven  $X_{\max}$  course with increasing energy. This is evident at energy 5 EeV, where the elongation rate of  $X_{\max}$  noticeably decreases. This is not contradicted by the data obtained in this work on muons.

Independent estimates of  $X_{\max}$  made from measurements of radio emission at the arrays in Yakutsk and LOFAR agree with the data obtained in the optical wavelength range and confirm the general behavior of the dependence of  $X_{\max}$  on energy.

Fig. 2b shows the Auger, Telescope Array and LOFAR data above 0.1 EeV and complex data on three components of the Yakutsk array: air shower Cherenkov light, muon component, and radio emission. An analysis of the general results shown in Fig. 2b indicates that the magnitude

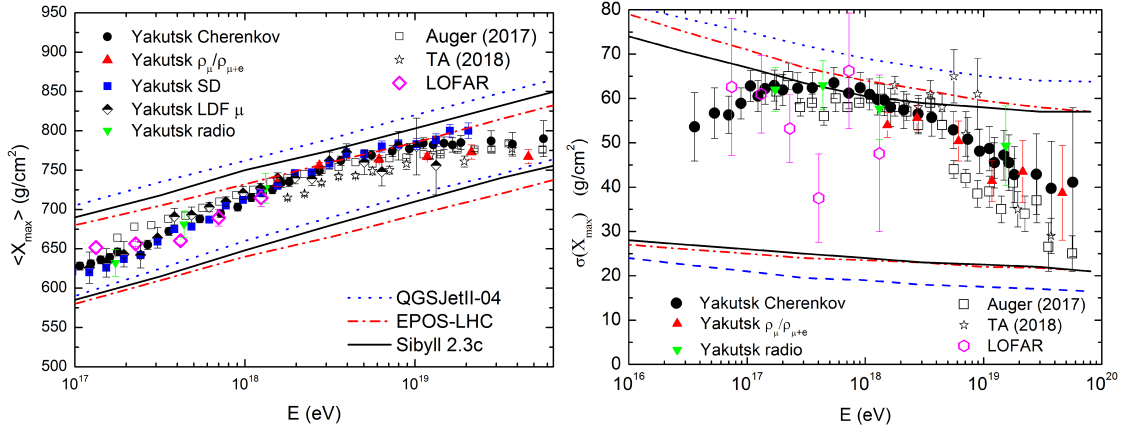


**Figure 2:** A) Dependence of the air shower depth of the maximum development  $X_{\max}$  on the energy  $E_0$ . The results of small and large air shower experiments are presented. The lines show the calculations by different models of hadronic interactions for the primary proton and the iron nucleus. B) dependence of fluctuations  $\sigma(X_{\max})$  on energy  $E_0$  and comparison with other experiments and model calculations.

of fluctuations  $X_{\max}$  is not constant over a wide range of energies. In the energy range 0.1-1 EeV, the value of fluctuations has a maximum value, which corresponds to the composition of cosmic rays, consisting of light nuclei — protons and helium nuclei. Beginning with energies of 5-8 EeV, fluctuations gradually decrease, which indicates a heavier composition of cosmic rays above these energies.

### 3. Mass Composition of cosmic rays in the region of highest energies

The CR MC  $\langle \ln A \rangle$  was estimated using interpolation formula (5) [15, 53].

$$\langle \ln A \rangle = \frac{X_{\max}^{\text{exp}} - X_{\max}^P}{X_{\max}^{\text{Fe}} - X_{\max}^P} \cdot \ln A_{\text{Fe}} \quad (5)$$

Here  $X_{\max}^P$  — depth of the maximum for a proton,  $X_{\max}^{\text{Fe}}$  — depth for the iron nucleus,  $X_{\max}^{\text{exp}}$  — depth of the maximum development of air shower according to the experimental data (Fig. 2a).  $\ln A_{\text{Fe}}$  is the natural logarithm of the atomic weight of iron.

The results of the Yakutsk array for  $\langle \ln A \rangle$  were obtained for four air shower components (Fig. 3) [26, 44, 54]. As can be seen from the figure, in the energy range of 5 EeV, the value of  $\langle \ln A \rangle$  begins to increase, which indicates an increase in the MC. For comparison, Fig. 3 shows the data from the Telescope Array [55], Auger [47], LOFAR [16] arrays. It can be seen that the results of the Telescope Array, Auger array for  $X_{\max}$  and  $\sigma(X_{\max})$  coincide with the results of the Yakutsk array in the region  $E_0 \geq 5$  EeV, including the results obtained for muons. The uncertainty associated with uncertainty of the real model of the development of air shower (by the example of muons), as can be seen from Fig. 3, cannot influence the conclusion about an increase in heavy nuclei in the cosmic ray flux, starting from energies of 30 EeV.

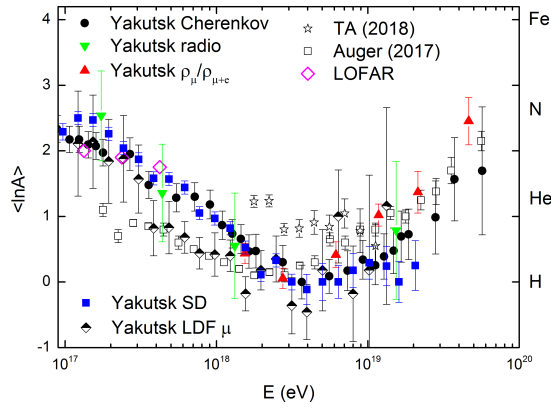


**Figure 3:** The mass composition of cosmic rays in the region of highest energies.

#### 4. Conclusion

In this work, an estimate of the depth of the maximum development was made, independent of the model of hadron interactions, by the parameter  $\rho_\mu(600)/\rho_{\mu+e}(600)$  in showers with energies above 5 EeV. The average values of  $\langle X_{\max} \rangle$  and their dependence on energy were found from the data in a wide range of energies (Fig. 2a).

Based on these data, an estimate of the CR MC was made above 5 EeV, which indicates a change in MC. This follows from a comparison of the experimental data  $X_{\max}$ ,  $\sigma X_{\max}$  and calculations using different models of hadronic interactions shown in Fig. 2a and Fig. 2b.

Using results of this work and results of other experiments [16, 47, 55] it can be concluded that CR MC consists of mix of light nuclei in energy interval 5-10 EeV (Fig. 2b, Fig. 3). It also indicated by fast displacement rate of  $X_{\max}$  to sea level  $ER = (63 \pm 5) g/cm^2$  (Fig. 2a), which is distinctive for mix of light nuclei — protons and helium nuclei.

For energies greater than 30 EeV, as can be seen from Fig. 3, CR MC starts to change to heavier elements — CNO and iron nuclei.

The independent MC results obtained by measuring air shower radio signals at the Yakutsk array [45] and the LOFAR [16] do not contradict these conclusions. It should be noted that the results obtained for MC are preliminary, because the models used do not fully reflect the real development of air shower, for example, in terms of muons. Discussions are currently underway on this issue [42].

#### References

- [1] V.L. Ginzburg. Modern Astrophysics (in Russian) (Atom, Moscow, 1970, 192)
- [2] V.L. Ginzburg. Phys. Uspekhi, **160**, No. 4, 419 (1999)
- [3] G.B. Gelmini, O.E. Kalashev and D.V. Semikoz, J. Exp. Theor. Phys. **106**, 1061 (2008).
- [4] P. Bhattacharjee and G. Sigl, Phys. Rep. **327**, 109 (2000).
- [5] F. Halzen & D. Hooper. Rep. Prog. Phys. **65**, 1025 (2002).

- [6] J.-T. Li, E. Hodges-Kluck, Ye. Stein et al., *ApJ* **837**, 27 (2019).
- [7] K. Mannheim, R.J. Protheroe and J.P. Rachen, *Phys. Rev. D* **63**, 023003 (2001).
- [8] H. Kang, D. Ryu and T.W. Jones, *ApJ* **456**, 422 (1996).
- [9] J.P. Rachen and P.L. Biermann, *A&A* **272**, 161 (1993).
- [10] E. Waxman, *Phys. Rev. Lett.* **75**, 386 (1995).
- [11] S.P. Knurenko, Z.E. Petrov and I.S. Petrov, *Physics of Atomic Nuclei* **82**, No. 6, 732 (2019).
- [12] R.U. Abbasi, M. Abe, T. Abu-Zayyad et al., *ApJ* **865**, 74 (2018).
- [13] R.U. Abbasi, M. Abe, T. Abu-Zayyad et al., *Astropart. Phys.* **80**, 131 (2016).
- [14] R.U. Abbasi, M. Abe, T. Abu-Zayyad et al., *ApJ* **909**, 178 (2021)
- [15] E.G. Berezhko, S.P. Knurenko and L.T. Ksenofontov, *Astropart. Phys.* **36**, 31 (2012).
- [16] S. Buitink, A. Corstanje and H. Falcke et al. *Nature* **531**, 70 (2016).
- [17] K-H. Kampert, M. Unger. *Astropart. Phys.* **35**, 660 (2012)
- [18] I.P. Ivanenko, I.D. Rapoport and V.Ya. Shestoporov. Energy spectrum and composition: cosmic rays with energy 2-100 TeV according to results of satellite “Kosmos-1713”. Scobeltsyn Nuclear Physics Research Institute. Moscow. 1988, 26 p.
- [19] N.L. Grigorov et al. *Cosmic research* **33**, No. 4, p. 339 (1995).
- [20] V.I. Zatsepin, M.I. Panasyuk, A.D. Panov, N.V. Sokolskaya, *Moscow University Physics Bulletin* **67**, N 6, 493 (2012)
- [21] O. Adriani, G. C. Barbarino, G. A. Bazilevskaya, et al., *Science* **332**, 69 (2011).
- [22] M. Aguilar, D. Aisa, B. Alpat et al., *Phys. Rev. Lett.* **114**, 171103 (2015).
- [23] D.M. Green and E.A. Hays, *PoS* **301**, 159 (2018).
- [24] A.D. Panov, J. H. Adams Jr., H. S. Ahn, et al., *Bull. Russ. Sci. Phys.* **73**, 564 (2009).
- [25] E. S. Seo, H. S. Ahn, P. Allison, et al., *Adv. Space Res.* **42**, 1656 (2008).
- [26] S. Knurenko and I. Petrov. *Adv. in Space Res.* **64**, 2570 (2019).
- [27] A. Aab, P. Abreu, M. Aglietta et al., *Nucl. Instrum. Meth A* **798**, 172 (2015).
- [28] T. Abu-Zayyad, R. Aida, M. Allen, et al., *Nucl. Instrum. Meth. A* **689**, 87 (2012).
- [29] S. Knurenko, A. Sabourov. *Astrophys. Space Sci. Trans.* **7**, 251 (2011)
- [30] S. P. Knurenko and I. S. Petrov. *Phys. Rev D* **102**, 023036 (2020).

- [31] J. Abraham, P. Abreu, M. Aglietta et al., Nucl. Instrum. Meth. A **613**, 29 (2010)
- [32] A.A. Atrashkevich, N.N. Kalmykov, G.B. Kristiansen, Pis'ma v ZhETF **33**, 236 (1981).
- [33] G.B. Khristiansen, Yu.A. Fomin, N.N. Kalmykov et al., Astropart. Phys. **2**, 127 (1994).
- [34] S. Knurenko, A. Ivanov and I. Slepsov, Nucl. Phys. B, Proc. Suppl. **196**, 391 (2009).
- [35] S. Ostapchenko, Phys. Rev. D **83**, 014018 (2011).
- [36] S.P. Knurenko and I.S. Petrov, JETP Lett. **107**, No. 11, 676 (2018).
- [37] M. Dyakonov, S. Knurenko, V. Kolosov et al., Nucl. Instrum. Meths. Phys. Res. A **248**, 224 (1986).
- [38] S. Knurenko, V. Kolosov, Z. Petrov, In: Proc. 27-th ICRC, Hamburg (Germany), **1**, 157 (2001).
- [39] A. Kochnev, In: Proc. of "Use of PC in control problems" Krasnoyarsk (USSR), 62 (1985).
- [40] D. Heck, J. Knapp, J. Capdevielle, G. Schatz and T. Thouw. CORSIKA: A Monte Carlo Code to Simulate Extensive Air Showers. FZKA 6019, (Forschungszentrum Karlsruhe, 1998, 90 p.)
- [41] A.V. Saburov. Spatial distribution of EAS particles with energy greater than 1017 eV by Yakutsk array data: dissertation. 01.04.16 / Institute of Nucl. Res., Moscow, 2017 – 146 p.
- [42] H.P. Dembinski et al., EPJ Web Conf., **210**, 02004 (2019).
- [43] A.V. Glushkov, A.V. Saburov. Phys.Atom.Nucl. **82**, 674 (2020)
- [44] S.P. Knurenko, Z.E. Petrov and I.S. Petrov, Nucl. Instrum. and Meth. in Phys. Res. A **866** 230 (2017).
- [45] I.S. Petrov, S. P. Knurenko and Z. E. Petrov, Phys. of Atom. Nucl. **82**, No. 6, 795 (2019).
- [46] A. Aab, P. Abreu and M. Aglietta et al. Phys. Rev. D **90**, 122006 (2014).
- [47] J. Bellido et al., Proc. Sci. **301**, 506 (2018).
- [48] R. U. Abbasi, M. Abe and T. Abu-Zayyad et al., Astropart. Phys. **64**, 49 (2015).
- [49] R. U. Abbasi, M. Abe and T. Abu-Zayyad et al., ApJ **865**, 74 (2018).
- [50] A. Corstanje et al., Proc. Sci. **395**, 322(2021)
- [51] F. Riehn, R. Engel, A.Fedynitch et al., Proc. Sci. **236**, 558 (2015).
- [52] T. Pierog, I. Karpenko, J. Katzy, Phys. Rev. C **92**, 034906 (2015).
- [53] J. Hörandel, J. Phys.: Conf. Ser., **47**, 41 (2006)
- [54] A.V. Glushkov, A.V. Sabourov, JETP Lett. **109**, 559 (2019)
- [55] R. U. Abbasi, M. Abe and T. Abu-Zayyad et al. Phys. Rev. D **99**, 022002 (2019)